# Seed-to-seedling transitions exhibit distance-dependent mortality but no strong spacing effects in a Neotropical forest

Philippe Marchand [ID],[1,8] Liza S. Comita,[2] S. Joseph Wright [ID],[3] Richard Condit,[4,5] Stephen P. Hubbell,[6] and Noelle G. Beckman [ID][7]

[1]*Institut de recherche sur les forêts, Université du Québec en Abitibi-Témiscamingue, Rouyn-Noranda, QC J9X 5E4 Canada*
[2]*School of Forestry & Environmental Studies, Yale University, New Haven, Connecticut 06511 USA*
[3]*Smithsonian Tropical Research Institute Panama City, 0843-03092 Panama*
[4]*Field Museum of Natural History Chicago, Illinois 60605 USA*
[5]*Morton Arboretum, Lisle, Illinois 60532 USA*
[6]*Department of Ecology and Evolutionary Biology, University of California, Los Angeles, California 90095 USA*
[7]*Department of Biology and Ecology Center Utah State University, Logan, Utah 84322 USA*

*Abstract.* Patterns of seed dispersal and seed mortality influence the spatial structure of plant communities and the local coexistence of competing species. Most seeds are dispersed in proximity to the parent tree, where mortality is also expected to be the highest, because of competition with siblings or the attraction of natural enemies. Whereas distance-dependent mortality in the seed-to-seedling transition was often observed in tropical forests, few studies have attempted to estimate the shape of the survival-distance curves, which determines whether the peak of seedling establishment occurs away from the parent tree (Janzen–Connell pattern) or if the peak attenuates but remains at the parent location (Hubbell pattern). In this study, we inferred the probability density of seed dispersal and two stages of seedling establishment (new recruits, and seedlings 20 cm or taller) with distance for 24 tree species present in the 50-ha Forest Dynamics Plot of Barro Colorado Island, Panama. Using data from seed traps, seedling survey quadrats, and tree-census records spanning the 1988–2014 period, we fit hierarchical Bayesian models including parameters for tree fecundity, the shape of the dispersal kernel, and overdispersion of seed or seedling counts. We combined predictions from multiple dispersal kernels to obtain more robust inferences. We find that Hubbell patterns are the most common and Janzen–Connell patterns are very rare among those species; that distance-dependent mortality may be stronger in the seed stage, in the early recruit stage, or comparable in both; and that species with larger seeds experience less overall mortality and less distance-dependent mortality. Finally, we describe how this modeling approach could be extended at a community scale to include less abundant species.

*Key words: dispersal kernel; Janzen–Connell hypothesis; seed dispersal; seedling establishment; species coexistence; tropical forest.*

## Introduction

The set of spatial processes occurring during the early life history stages of a plant's life are hypothesized to play a major role in population dynamics (Beckman et al., 2019, Howe and Miriti, 2004, Schupp, et al., 2010) and local coexistence of plant species (Janzen, 1970, Hubbell, 1980, Beckman and Rogers, 2013). During these early life history stages, plants have the ability to change their geographic location through seed dispersal and experience their highest mortality. Seed dispersal influences recruitment through the seedscape — the biotic and abiotic factors surrounding a seed (Beckman and

Rogers, 2013) — and sets the initial spatial template of plants Nathan and Muller-Landau, 2000). If negative density- or distance-dependent processes are strong, mortality is expected to be highest underneath the parent tree where seed densities also tend be the highest (Janzen, 1970). This may be due to competition with siblings or mortality due to specialized natural enemies that are either attracted to the parent tree or the high seed densities (Janzen, 1970, Connell, 1971). A recent meta-analysis of experimental studies provides evidence for negative distance- or density-dependent mortality in plant communities worldwide, as predicted by the Janzen–Connell hypothesis (Comita et al., 2014). Alternatively, survival may be increased under the tree due to increased suitability of the habitat, satiation of seed predators (Nathan and Casagrandi, 2004), or presence of root mutualisms on the parent tree (McCanny, 1985). All of these processes result in a spatial signature that

[8]E-mail: philippe.marchand@uqat.ca

can be observed in the distribution of seeds and surviving seedlings with respect to the location of the parent plants. Given the link between seed densities and distance from parent trees, it is difficult to separate the effects of distance-dependent processes from those of density-dependent processes in observational studies. We therefore often refer to "distance-/density-dependent" processes in the text, whereas the separate use of "distance-dependence" or "density-dependence" indicates that the result reported focuses on that specific type of pattern.

We can characterize the seedling recruitment pattern by describing the spatial patterns of seed dispersal, survivorship, and seedling establishment. The seed-dispersal kernel, representing the two-dimensional probability density of seed fall relative to the parent tree, tends to show a monotonic decline with distance (Muller-Landau et al., 2008, Bullock et al., 2017). The product of the seed dispersal kernel with the (potentially distance-/density-dependent) probability of survival to the seedling stage is known as the seedling establishment or effective dispersal kernel (Nathan et al., 2012). The interaction between the dispersal and survival functions leads to different predicted forms of the seedling establishment kernel, as reviewed in Nathan and Casagrandi (2004). In all cases, seed dispersal is assumed to decrease monotonically with distance. If seedling survival also decreases with distance, the seedling establishment kernel will show a steeper decline (shorter tail) than the seed dispersal kernel (McCanny pattern). Distance-independent survival results in identical kernels for seed dispersal and seedling establishment. If survival increases with distance but does not compensate for the decrease in seed density, the seedling establishment kernel will be monotonically decreasing, but with a longer tail (Hubbell pattern). Finally, a steeper increase of survival with distance can result in a maximal seedling density away from the parent tree, producing the hump-shaped Janzen–Connell pattern (Fig. 1).

Most studies of spatial patterns in tree communities have focused on the dispersal of seeds (Levin et al., 2003, Muller-Landau et al., 2008) or the spatial organization of juvenile and mature individuals (Wiegand et al., 2009, Lin et al., 2011, Murphy et al., 2017), whereas studies of the shifts in spatial patterns in the seed-to-seedling transition remain comparatively rare. Such studies may proceed by comparing the density of seeds and seedlings in co located sampling plots, for example, as in Swamy et al. (2011), who found evidence for declining survivorship in proximity to conspecific trees for 15 Amazonian tree species. In order not only to detect instances of distance-dependent recruitment, but also to distinguish the possible recruitment patterns described above, we need a direct characterization of the shape of the seed dispersal and seedling establishment kernels with respect to focal parent trees in a natural community.

In this study, we estimate the seed-dispersal kernels and seedling establishment kernels for several Neotropical tree species from multi year seed and seedling surveys at Barro Colorado Island (BCI), Panama. We consider seedling establishment at two stages (new recruits and seedlings 20 cm or taller) to distinguish mortality in the seed-to-seedling transition from that of the early seedling life. Previous studies at the same site have characterized interspecific variation in seed dispersal kernels (Muller-Landau et al., 2008), found evidence for negative density dependence on seedling recruitment (Harms et al., 2000, Wright et al., 2005b), as well as distance-/density-dependent mortality during the seedling stage (Comita et al., 2010, Murphy et al., 2017), but see Detto et al. (2019) for discussion of potential biases in some of these studies. Drawing from the approach of Muller-Landau et al. (2008), we fit hierarchical Bayesian models for each species and life stage (seed, new recruit, and 20-cm seedling) to estimate the annual fecundity (total seeds or seedlings per unit of reproductive tree basal area), the seed dispersal or seedling establishment kernel, and the spatial aggregation of individuals relative to expected density simultaneously. We hypothesize that species for which survival increases with distance, as evidenced by Hubbell or Janzen–Connell recruitment patterns, will show a reduction in spatial aggregation from the seed to seedling stage. As previous studies have shown that the negative effect of conspecific density on seedling survival was reduced for species with greater seed mass (Lebrija-Trejos et al., 2016) and for the more abundant species at BCI (Comita et al., 2010), we hypothesize that the survival of these species' seedlings will also be less distance dependent.
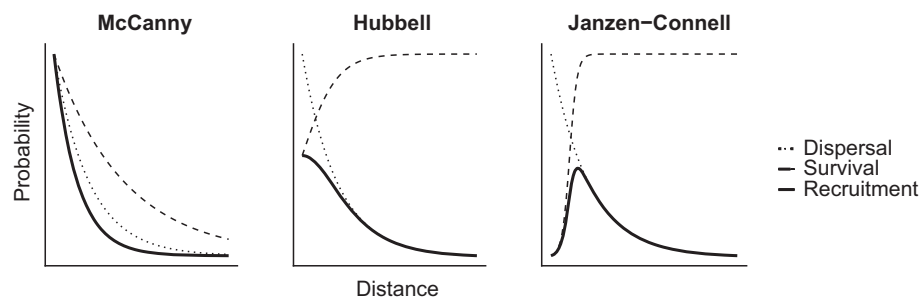


Fig. 1. Illustration of McCanny, Hubbell, and Janzen–Connell patterns of seedling recruitment based on the shape of the dispersal kernel and the survival probability as a function of distance Nathan and Casagrandi, 2004).

## METHODS

### Study site

This analysis was conducted on data collected from the 50-ha CTFS forest dynamics plot (referred to from this point on as the study area) on Barro Colorado Island (9°10′N, 79°51′W), a 1,600-ha island located in Gatun Lake in central Panama (Hubbell and Foster, 1983, Condit, 1998). It is a lowland, moist tropical forest, with average annual rainfall of 2,600 mm (Leigh et al., 1996, Paton, 2007) and a dry season extending from around mid-December to the end of April.

### Tree, seed, and seedling data

To determine the distribution of adult trees in the study area, we used data from tree censuses conducted in 1982 and every 5 yr from 1985 to 2015 (Condit et al., 2012). Each census includes the species, coordinates (precise to 0.5 m), and diameter at breast height (DBH, measured at 1.3 m above the ground) for all free-standing woody plants having a DBH ≥ 1 cm (Condit, 1998, Hubbell et al., 1999).

We interpolated the distribution of trees and their basal areas between census years. If a tree was alive in census year $y_1$ and dead in year $y_2$, we assumed a uniform probability of survival over the intermediate years $y$ ($y_1 < y < y_2$):

$$P(\text{alive at } y) = \frac{y_2 - y}{y_2 - y_1}. \tag{1}$$

Basal area ($b$) was calculated from the DBH and, when applicable, interpolated between years assuming geometric growth; that is

$$b_y = b_{y1}\left(\frac{b_{y_2}}{b_{y_1}}\right)^{\frac{y-y_1}{y_2-y_1}}. \tag{2}$$

We excluded trees with a DBH under a minimum reproductive threshold. Following Muller-Landau et al. (2008) that minimum DBH was set as 2/3 of the reproductive size thresholds estimated by Robin B. Foster (reported in Wright et al., 2005a). The more permissive threshold corresponds to the inflection point of logistic regressions of reproductive status against DBH, which were tightly clustered around 2/3 of the Foster estimates, and further motivated by the finding that excluding reproductive trees has a larger impact on the dispersal kernel estimates than including non reproductive trees (Muller-Landau et al., 2008).

The seed-dispersal models were fitted using 27 yr (1988–2014) of seed-fall data collected from 450 seed traps set along the study area trails. Two hundred traps were present during the whole period and the 250 others were added at various points in time, for a total of 6,388 trap-years. The seed traps were formed by a 0.5-m² PVC frame attached to a 1-mm mesh bag, suspended 0.8 m above the ground by PVC posts. Seed, fruit, and other reproductive parts of trees that fell in the traps were identified to species and counted on a weekly basis (Wright and Calderon, 1995, Wright et al., 1999). The seed counts input to the models were the sum of individual seeds and seeds from mature fruits caught in the traps, the latter obtained by multiplying fruit counts to species-specific seed-to-fruit ratios (S. J. Wright, *unpublished data*). Seed-to-fruit ratios were calculated by taking the mean of five mature fruits from five individuals of each species. Seed masses were obtained as described in Wright et al. (2010).

The seedling establishment models are based on two data sources. The first, which we refer to as the "recruit" data set, includes counts of new recruits by species in 800 1-m² quadrats located around 250 of the seed traps (three or four quadrats per trap), for a total of 14,952 quadrat-years in the 1994–2014 period (Wright et al., 2005b). Seed and recruit counts were matched by year, accounting for species-specific seasonal variation in seed production and germination delays (S. J. Wright, *unpublished code*). The second seedling data set, which we refer to as the "20-cm seedling" data set, is composed of seedling counts from 20,000 1-m² quadrats set in a 5 × 5 m grid across the study area. Ten seedling censuses were performed in the 2001–2013 period (annually except for 2005, 2007, and 2010), where all woody plants <1 cm in DBH and at least 20 cm in height were tagged, mapped, and identified to species (Comita et al., 2007a). To estimate annual recruitment into this size class, we counted new individuals in the seedling quadrats for the nine intervals between the 10 census years. For the 2-yr intervals (2004–2006, 2006–2008, 2009–2011), we divided the raw counts by two; fractional values were randomly rounded up or down. Because of the lack of knowledge of individuals' ages, seedlings in that second data set cannot be tied to a specific seed production year.

To minimize the contribution of uncensused trees from outside the study area, we excluded 29 seed traps located less than 20 m from the area boundary, along with their associated recruit quadrats. Because the purpose of this study is to compare seedling establishment curves with the corresponding seed-dispersal kernels, we also subset the 20-cm seedling data to the 1,700 quadrats located within 10 m of one of the remaining seed traps. This distance threshold was chosen to minimize sampling location bias in comparing the two data sets, while maintaining a sufficient seedling sample size.

For this analysis, we selected monoecious tree species Bruijning et al., 2017) with a reproductive DBH threshold of 2 cm or greater. To study the seed-to-recruit transition, we selected 27 species with seeds found in at least 125 trap-years and recruits found in at least 45 quadrat-years (Table 1). For the recruit-to-20-cm seedling transition, we considered 12 of those 27 species with at least 30 20-cm seedlings in the final data set. Because of

TABLE 1.   Tree species modeled in this study.

| Species | RDBH (cm) | Disp. mode | SF ratio | Trees | Seeds | Recruits | Seedlings (≥20 cm) |
|---|---|---|---|---|---|---|---|
| *Alseis blackiana* | 13.3 | W | 28.2 | 1,018 | 2,979,232 | 119 | 63 |
| *Apeiba membranacea* | 20.0 | A | 171.1 | 191 | 246,99 | 130 | |
| *Beilschmiedia tovarensis* | 20.0 | A | 1.0 | 225 | 2,330 | 1,969 | 1,133 |
| *Brosimum alicastrum* | 20.0 | A | 1.0 | 97 | 103,58 | 139 | 108 |
| *Chrysophyllum cainito* | 20.0 | A | 3.0 | 20 | 1,713 | 241 | 38 |
| *Cordia alliodora* | 13.3 | W | 1.0 | 94 | 6,483 | 213 | |
| *Cordia bicolor* | 10.7 | A | 1.0 | 473 | 7,871 | 83 | 34 |
| *Cordia lasiocalyx* | 6.7 | A | 1.0 | 1,021 | 1,351 | 82 | |
| *Coussarea curvigemmia* | 2.0 | A | 1.0 | 2,148 | 1,155 | 113 | |
| *Dendropanax arboreus* | 20.0 | A | 5.3 | 83 | 10,472 | 227 | |
| *Desmopsis panamensis* | 2.0 | A | 5.1 | 12,574 | 1,351 | 481 | |
| *Eugenia oerstediana* | 13.3 | A | 1.0 | 212 | 2,369 | 967 | 330 |
| *Guatteria lucens* | 20.0 | A | 1.0 | 175 | 2,103 | 80 | |
| *Gustavia superba* | 6.7 | A | 12.2 | 764 | 1,288 | 445 | 106 |
| *Handroanthus guayacan* | 20.0 | W | 1.0 | 29 | 4,531 | 205 | |
| *Hasseltia floribunda* | 5.3 | A | 1.2 | 620 | 3,656 | 87 | |
| *Heisteria concinna* | 10.0 | A | 1.0 | 406 | 1,138 | 651 | 48 |
| *Hirtella triandra* | 5.3 | A | 1.0 | 2,143 | 1,028 | 266 | 57 |
| *Inga marginata* | 20.0 | A | 1.0 | 154 | 1,167 | 795 | 266 |
| *Jacaranda copaia* | 20.0 | W | 245.4 | 256 | 177,563 | 151 | |
| *Lacmellea panamensis* | 10.7 | A | 2.0 | 67 | 292 | 146 | |
| *Luehea seemannii* | 20.0 | W | 43.1 | 77 | 289,443 | 211 | |
| *Poulsenia armata* | 20.0 | A | 6.2 | 329 | 1,042 | 92 | |
| *Quararibea asterolepis* | 20.0 | A | 1.7 | 655 | 34,806 | 1,507 | 200 |
| *Tabebuia rosea* | 20.0 | W | 146.6 | 47 | 5,515 | 234 | |
| *Tabernaemontana arborea* | 20.0 | A | 34.6 | 349 | 2,210 | 71 | |
| *Unonopsis pittieri* | 5.3 | A | 1.0 | 438 | 940 | 71 | 34 |

*Notes:* The last four columns are the counts of reproductive trees, seeds (fruits counted as seed equivalents), recruits, and seedlings (20 cm or taller) of the species across all years. Seedling counts below the study inclusion threshold are not shown.

Disp. mode, Dispersal by animals (A) or wind (W); RDBH, estimated minimal DBH for reproduction; SF ratio, average seeds per fruit ratio.

computational limitations, we could not fit any models to species with >20,000 reproductive trees, which excluded *Faramea occidentalis* and could not fit the 20-cm–seedling model to species with >10,000 trees, which excluded *Desmopsis panamensis*.

### Estimation of dispersal kernels

Similar to Muller-Landau et al. (2008), we used a hierarchical Bayesian model to jointly estimate fecundity and dispersal parameters for a series of candidate dispersal models jointly. The Bayesian approach provides two main benefits for this problem: (1) prior distributions can be chosen to enforce weak physical constraints on the dispersal kernels and avoid unrealistic dispersal distances (see the following and Appendix S2); and (2) the analysis outputs samples from the joint posterior distribution of all model parameters, from which we can calculate the posterior distribution of any derived quantity of interest (e.g., mean dispersal distance).

For brevity, the model structure is described here in terms of seed-trap data, but the same equations apply to the recruit and 20-cm seedling data. Separate models were fit for each tree species.

The model calculates the expected number of seeds in trap $j$ and year $y$ ($\hat{S}_{jy}$) as the sum of contributions from each conspecific reproductive tree within the 50-ha study area, plus an estimate of the contribution from trees outside the area. If the fecundity (total seed output) from tree $i$ in year $y$ is a function $Q_y$ of its basal area $b_{iy}$, and the probability of a seed from tree $i$ being dispersed to the location of trap $j$ is given by the dispersal kernel $F$ ($r_{ij}$), the expected number of seeds from trees of a given species in the study area (ISA) is

$$\hat{S}_{jy(\text{ISA})} = a_p \sum_i Q_y(b_{iy}) F(r_{ij}), \qquad (3)$$

where $a_p$ is the area of a seed trap. Note that $F$, although isotropic, represents a two-dimensional (probability per unit area) rather than a one-dimensional (radial) kernel. We assumed this kernel was fixed in time and thus represented the average dispersal pattern for the species, but allowed inter annual variation in the fecundity function $Q$. Muller-Landau et al. (2008) estimated the contribution of uncensused trees by integrating the dispersal kernel outside the study area (OSA), assuming seed production per unit area was uniform and equal to the

total fecundity of all censused trees of the species divided by the size $a_s$ of the study area:

$$\hat{S}_{jy(\text{OSA})} = a_p \frac{\sum_i Q_y(b_{iy})}{a_s} \int_{\phi=0}^{2\pi} \int_{r_{0j}(\phi)}^{\infty} F(r)r\,dr\,d\phi. \quad (4)$$

The integral in Eq. 4 is expressed in polar coordinates, with $r_{0j}(\varphi)$ being the distance from trap $j$ to the edge of the study area in direction $\varphi$. Because it depends on direction, the calculation does not simplify to a radial integral and, for most kernels, requires numerical integration. To avoid spending most of the computational effort on those marginal seed sources, we changed the lower bound of the integral in Eq. 4 to $r_{j\,\text{max}}$, which is the maximum of $r_{0j}$ across all directions $\varphi$. This leaves out the contributions of areas outside the rectangular plot but within $r_{j\,\text{max}}$. To account for these, we applied a weighted edge correction (Ripley, 1977, Perry et al., 2006) to Eq. 3 for the contribution of censused trees inside the study area. For tree $i$ and trap $j$, the weight $w_{ij}$ is the inverse of the proportion of the circle of radius $r_{ij}$, centered at $j$, that overlaps the study area. Therefore $w_{ij} \geq 1$, with the equality meaning that the circle is entirely within the study area.

In summary, the expected number of seeds in trap $j$ in year $y$ was calculated per species as

$$\hat{S}_{jy} = a_p \left( \sum_i Q_y(b_{iy}) w_{ij} F(r_{ij}) + \frac{\sum_i Q_y(b_{iy})}{a_s} \int_{r_{j\text{max}}}^{\infty} F(r) 2\pi r\,dr \right). \quad (5)$$

We modeled fecundity as proportional to the basal area Ribbens et al., 1994; Clark et al., 1998, 1999; Muller-Landau et al., 2008):

$$Q_y(b_{iy}) = \exp(\beta_y)b_{iy}. \quad (6)$$

We assumed that the variation in $\beta_y$, the logarithm of the proportionality factor, is normally distributed across years with a mean $\mu_\beta$ and a standard deviation $\sigma_\beta$. Note that $b_{iy}$ has units of centimeters squared in this paper and thus $\exp(\beta_y)$ has units of seeds/cm$^2$. Other distances, areas and densities in Eq. 5 are based on meters.

We evaluated five functional forms for the dispersal kernel: the 2D $t$ (Clark et al., 1999), exponential power (Clark et al., 1998), log-normal and Weibull distributions, as well as an inverse power law (Nathan et al., 2012). The probability density functions, cumulative distribution functions, and summary statistics for those distributions are listed in Appendix S1.

We considered two distributions for the observed seed counts, $S_{jy}$: a Poisson distribution with mean $\hat{S}_{jy}$, or a negative binomial with mean $\hat{S}_{jy}$ and dispersion parameter $\theta$ (Clark et al., 1998). The variance of the negative binomial distribution is equal to $\hat{S}_{jy} + \hat{S}_{jy}^2/\theta$. Smaller

values of $\theta$ indicate a greater degree of aggregation of the counts per trap; thus $1/\theta$ can be seen as a measure of clumping. In the Poisson limit, $1/\theta \rightarrow 0$.

The selection of prior distributions for all model parameters is described in Appendix S2. With limited seed rain data very close or very far from parent trees, unconstrained model fits can lead to extremely leptokurtic (heavy-tailed) kernels; thus it is usually necessary to apply prior constraints on kernel parameters (Clark et al., 1999). Therefore, we chose weakly informative priors for dispersal kernel parameters, so that most of the prior weight would result in reasonable values of the median and mean dispersal distances (i.e., 1–500-m range). We checked that the model parameters were identifiable by applying the model-fitting procedure to data sets simulated from the priors (Appendix S2).

We fit the models using the Hamiltonian Monte Carlo (HMC) software Stan (Carpenter et al., 2017). In order to assess convergence, two HMC chains were run for each model, with 600 warmup steps and 1,000 sampling steps per chain.

### Model evaluation and multimodel estimates

We obtained 10 model fits (five kernels × two count distributions) per species and life stage (seed, recruit, and 20-cm seedling). Based on recommended HMC diagnostics (Betancourt, 2017), we rejected models where more than one iteration was divergent or reached maximum tree depth, and models with a Bayesian fraction of missing information (BFMI) <0.2. We verified that the Gelman–Rubin convergence statistic $\hat{R} < 1.1$ for all valid models, indicating good mixing of the two HMC chains (Gelman and Rubin, 1992). After confirming convergence, we merged the posterior samples from the two chains for analysis, resulting in 2,000 samples per model.

We characterized the goodness-of-fit of valid models by comparing summary statistics of the observed data to those of data sets simulated from each posterior sample (posterior predictive checks). We considered three summary statistics: the summed log-likelihood of the data, the summed counts in all trap-years, and the total number of trap-years with non zero counts. Models where the observed statistic was in the extreme 2.5% on either side of the posterior distribution or, in the case of the likelihood, in the bottom 5% were excluded because of poor fit.

For each species and life stage, we computed multimodel posterior predictions for the dispersal kernel shape ($F(r)$ for a series of values of $r$), as well as the modal, median, and mean dispersal distance. We extracted a posterior predictive distribution from each model passing the diagnostic and goodness-of-fit tests, then created a multimodel posterior by resampling each distribution with weights estimated by model stacking (Yao et al., 2018). Model stacking finds a vector of weights for candidate models that maximizes some measure of out-of-sample predictive ability, in this case, the

expected predictive density of leave-one-out cross-validation. We used the method of Vehtari et al. (2017), as implemented in the R package *loo*, which produces estimates of that metric without the computational cost of computing cross-validation folds. Multimodel estimates were based on the minimal model set containing >95% of the cumulative weight per species and life stage. We also computed multimodel estimates of the fecundity parameters ($\mu_\beta$, $\sigma_\beta$) and clumping factor ($\theta^{-1/2}$) using the same stacking weights; the clumping factor was set at 0 for Poisson models.

### Survival estimates

For a series of distances $r$, we calculated relative survival (up to a distance-independent constant) in the seed to recruit transition as the ratio of $F_{recruit}(r)$ and $F_{seed}(r)$, with a similar calculation for the recruit-to-20-cm seedling transition. We obtained multimodel posterior distributions of relative survival for each $r$ by taking the ratios of randomly paired values from the multimodel distribution of the dispersal kernels described in the previous section.

We use the ratio of median relative survival at 50 vs. 5 m as a measure of strength of distance-dependent effects on survival. We set a lower bound at 5 m because some of the rarer species had very few (<5) reproductive individuals within 5 m of a seed trap, substantially increasing the uncertainty of survival estimates at small distances. The upper bound was set at 50 m to facilitate comparison with the strength of distance-dependent effects estimated by Murphy et al. (2017) for seedlings 20 cm and taller: in that study, the strength of distance-dependence was calculated as the standardized deviation from expected seedling survival rates, averaged over distances 0–50 m from conspecific mature trees.

In addition to estimating relative, distance-dependent survival, we obtained estimates of absolute, distance-independent survival from the estimated fecundity parameters. Using the median point estimates of $\mu_\beta$ and $\sigma_\beta$ by species and life stage, we estimated the mean production of seeds, recruits, or 20-cm seedlings per basal area as $\exp\left(\hat{\mu}_\beta + \hat{\sigma}_\beta^2/2\right)$, then considered the ratio of these estimates for recruits and seeds (respectively, 20-cm seedlings and recruits) as estimates of overall survival rates.

### Results

### Model evaluation

The complete list of model diagnostics, goodness-of-fit checks, and multimodel averaging weights can be found in Data S1: model_evaluation_table.csv. One of the 10 model versions, with log-normal dispersal kernel and Poisson counts, failed HMC diagnostics for every species and life stage. The nine other model versions passed diagnostics for 24 of 27 species at the seed stage and 21 of 27

species at the recruit stage. The remaining species (three for seeds and six for recruits) had failures for 1–5 of the nine models. At the 20-cm seedling stage, 1–8 models failed depending on the species. All models passing the HMC diagnostics had $\hat{R} < 1.05$ for all parameters.

After excluding models with poor goodness-of-fit and calculating stacking weights, the final candidate set (>95% cumulative weight) contained two or three models for most species at the seed and recruit stage, and typically more (up to seven) at the 20-cm seedling stage: this may be a reflection of the sparser data at the latter stage. For the seed stage, only models with negative binomial counts passed the goodness-of-fit checks.

We excluded a few species from further analysis because of a lack of valid models for either seeds or recruits. For two species with large numbers of wind-dispersed seeds, *Jacaranda copaia* and *Luehea seemannii*, fitted seed-dispersal models overestimated total seed counts while underestimating non zero counts. For *Lacmellea panamensis*, the best-fitting model for recruits had a very narrow dispersal kernel centered on $r \sim 500$ m, which would nearly exclude trees in the study area as potential parents. Finally, *Beilschmiedia tovarensis* was excluded for the 20-cm seedling stage only, as fitted models overestimated non zero counts.

### Characterization of the dispersal kernels

For most species, the estimated dispersal kernels at consecutive life stages either overlap or show a Hubbell pattern, characterized by slower distance decay for the later stage (Fig. 2). Only the recruit kernels for *Alseis blackiana* and *Dendropanax arboreus* show a non zero mode near 10 m, indicative of a Janzen–Connell pattern. However, many recruit and 20-cm seedling kernels display large uncertainty at small $r$, because of the rarity of parent trees near traps; therefore, it may be difficult to detect a mode at a small but non zero distance for those species.

For all modeled species, the median dispersal distance is comparable or greater for new recruits compared to seeds, and (when applicable) for 20-cm seedlings compared to new recruits (Fig. 3), consistent with greater mortality closer to parent trees. Three species (*Coussarea curvigemmia*, *Eugenia oerstediana*, and *Inga marginata*) have very large (>1 km) and uncertain estimates for the mean seed dispersal distance, as would be expected for very heavy-tailed kernels.

### Seed and recruit survival

For most species, the estimated survival rate monotonically increases by one or two orders of magnitude across the 1–100-m range for either or both transitions (seed to recruit, recruit to 20-cm seedling). Exceptions include *B. tovarensis* and *D. panamensis*, which experience decreased survivorship for $r > 5$ m, and *Handroanthus guayacan*, for which survivorship decreases from 1 to 10 m (Fig. 4). Three species show a more drastic
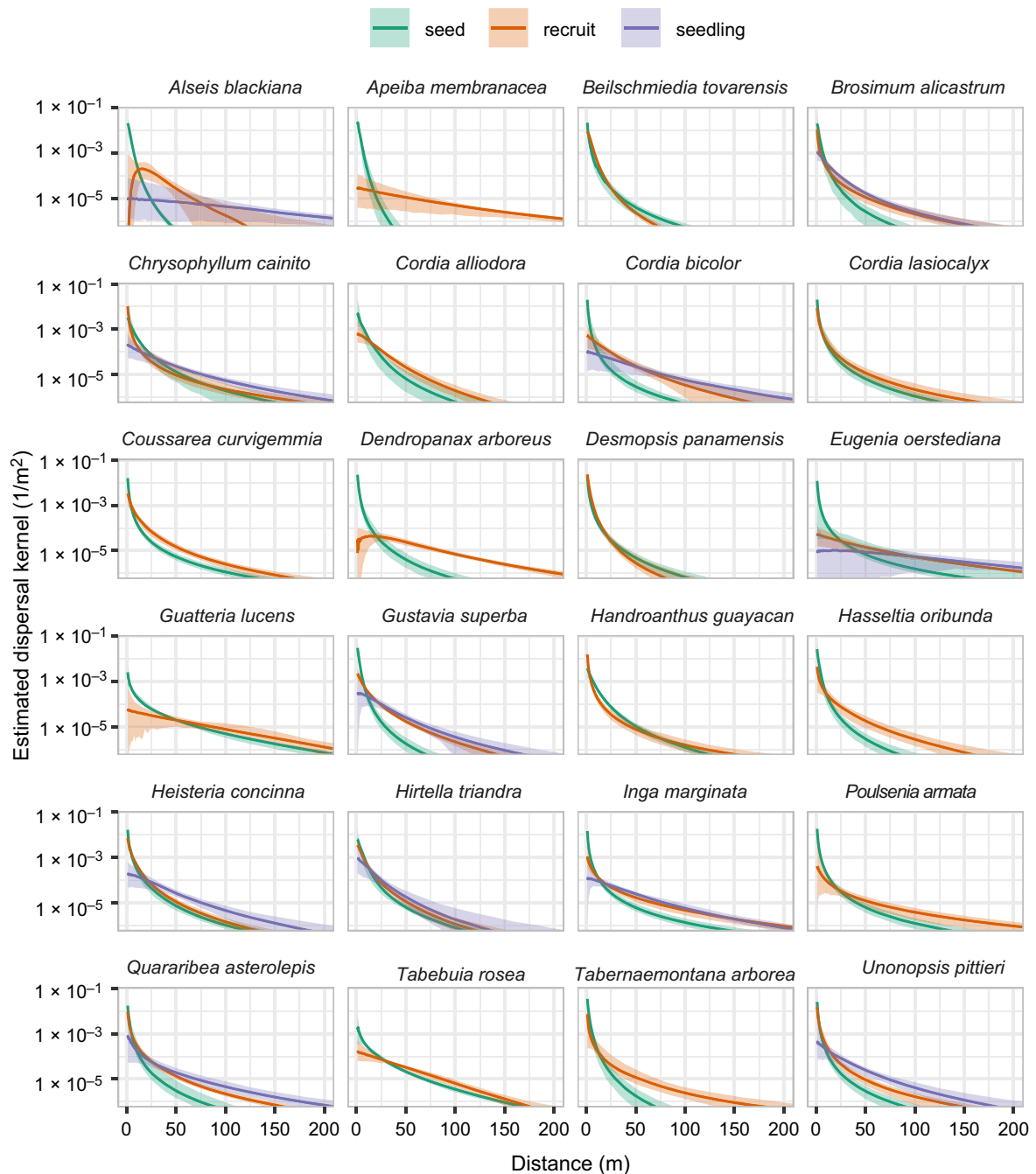
Fig. 2. Posterior estimate of the two-dimensional dispersal kernel (probability density of individuals per unit area at given distance of parent) by life stage and species. The median estimates (solid line) and 95% Bayesian credible intervals (shaded area) were calculated at 50 points from distances of 1–200 m from the multimodel posterior distributions, as described in the text.

increase in seed-to-recruit survival from 1 to 100 m: four orders of magnitude for *D. arboreus*, six for *Apeiba membranacea*, and eight for *A. blackiana*. The latter could be explained by the very high (~50,000) ratio of seed to recruit densities in the data set.

Seed mass is positively correlated with overall survival rate and negatively correlated with the strength of distance-dependent survival (relative survival at 50 vs.

5 m) for the seed-to-recruit transition. There is no significant correlation between seed mass and survival in the recruit to 20-cm seedling transition. The abundance of mature trees is not correlated with survival at any stage (Fig. 5).

Among the 14 species present in both this study and that of Murphy et al. (2017), we found no correlation between the strength of distance-dependent survival
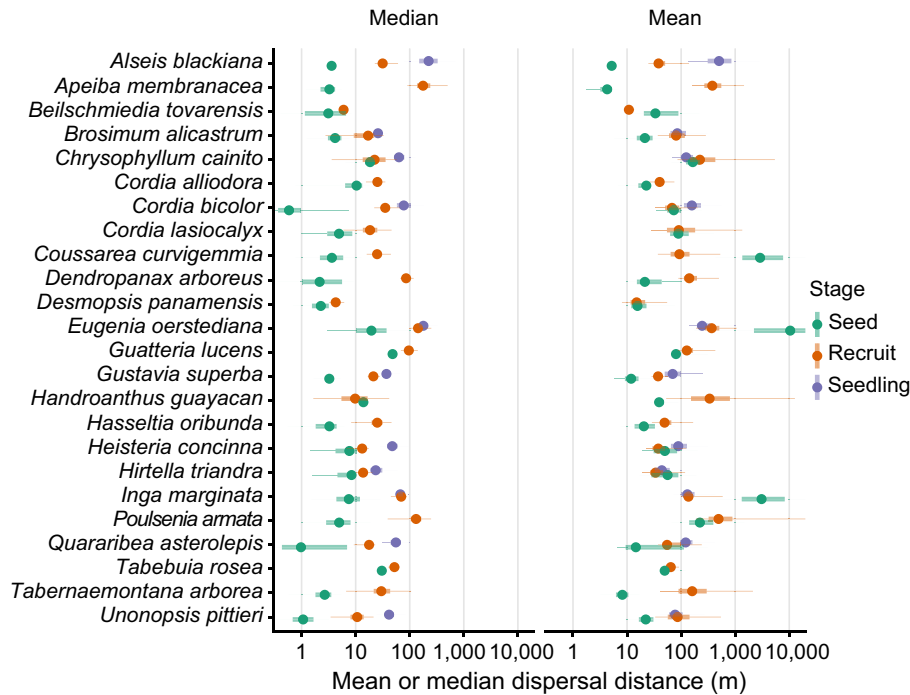
FIG. 3. Median, 50% credible interval (thick line) and 95% credible interval (thin line) of the multimodel posterior distribution of the median and mean dispersal distance by species and life stage.

estimated in this study, from the seed to the 20-cm seedling class, and the strength of distance-dependent survival estimated by Murphy et al. (2017) for seedlings 20 cm or taller (Appendix S3: Fig. S4). We also found no evidence that species experiencing greater distance-dependent mortality became less clumped in later life stages (Appendix S3: Fig. S5); in fact, smaller seeds were associated with both greater distance-dependent mortality and higher clumping in the recruit stage compared with the seed stage (Fig. 5).

The fecundity and clumping parameter estimates per species and life stage can be found in the supplementary materials (Appendix S3: Figs. S1–S3).

DISCUSSION

By comparing estimated kernels of seed dispersal and seedling recruitment for 24 common species in the BCI forest dynamics plot, we have shown that, although survival in the seed-to-seedling transition generally increases with distance from potential parent trees, the strength of this effect does not generate significant spacing between the seed-dispersal and seedling-recruitment density peaks. According to the classification of Nathan and Casagrandi (2004), we thus observed Hubbell rather than Janzen–Connell patterns of distance dependence. Nathan and Casagrandi (2004) hypothesize that Hubbell patterns can emerge from mobile predators that distribute themselves according to an ideal free distribution and that these predators may tend to be generalists.

These results do not contradict reports of strong recruitment suppression of older seedlings and saplings near conspecific adult trees (e.g., Swamy et al., 2011), as seedling density peaks can move away from conspecific adults during the seedling stage (Murphy et al., 2017). The lack of a consistent relationship between the strength of distance-dependence measured by Murphy et al. (2017) and that estimated here for the same species suggest that different pressures apply in the seed-to-seedling transition compared with the later seedling stage.

In line with prior studies (Lebrija-Trejos et al., 2016) we found that seed mass was positively correlated with seed survival independent of distance, as well as negatively correlated with distance-dependent seed mortality. Whereas Comita et al. (2010) found that more abundant species experienced less density-dependent mortality, we did not find any correlation between distance-dependent mortality and abundance; however, the former study considered the survival of seedlings 20 cm or taller and included a greater number of species with a wider range of abundance through a hierarchical model. Therefore, a limitation of our current study is that we could only include the most abundant species, and such species may be less sensitive to distance- or density-dependent mechanisms compared to less common species.

Contrary to our expectations, recruit clumping did not decrease for seeds experiencing greater distance-dependent mortality, and recruits were more clumped than seeds for species with small seeds. In our model, the
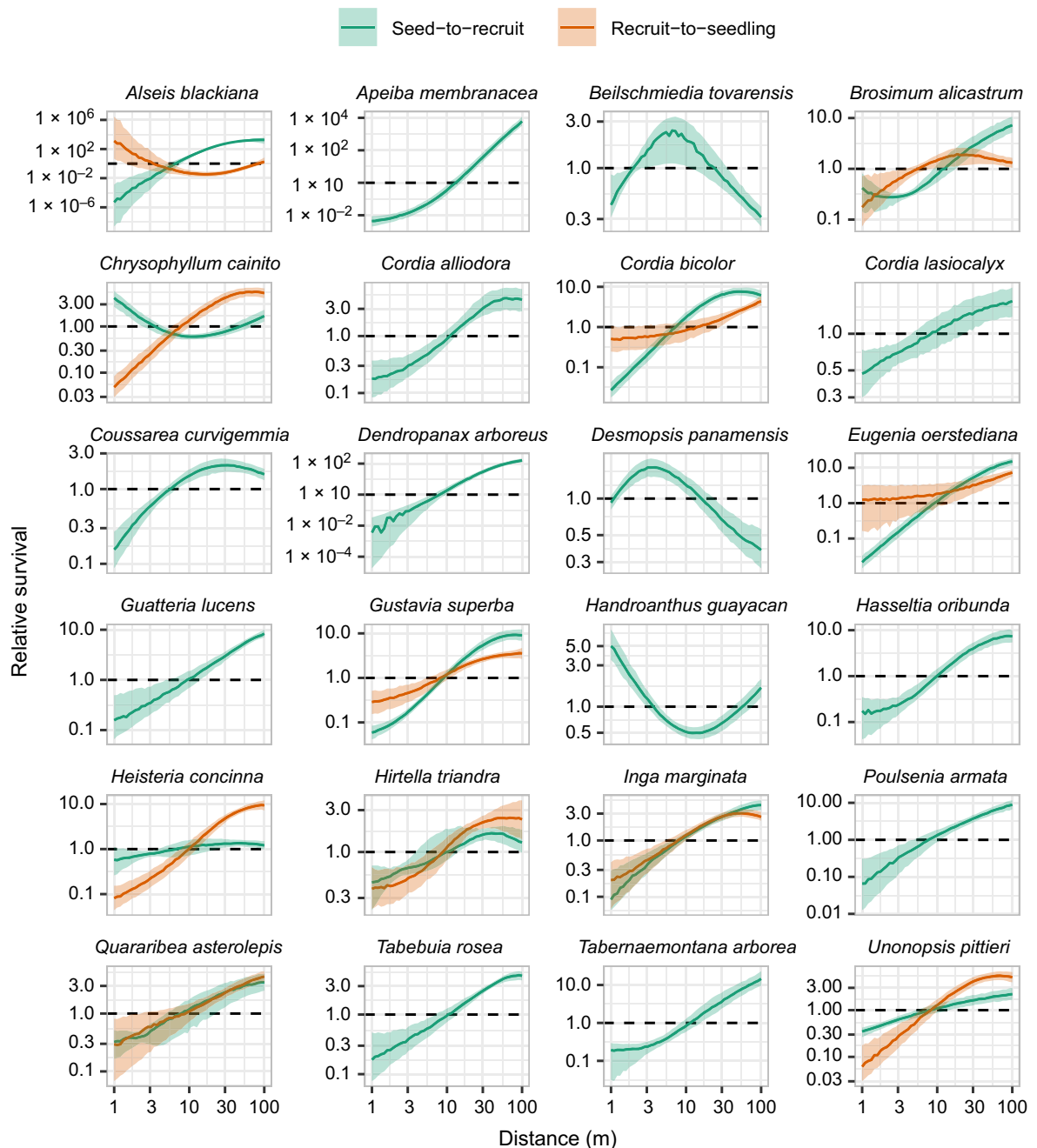
FIG. 4. Median (solid line) and 50% credible interval (shaded area) of the relative probability of survival, calculated as the ratio of new recruit and seed kernels, or 20-cm seedling and recruit kernels, as a function of dispersal distance $r$. Each curve is scaled to a median of 1 across the range of distances considered.

clumping parameter accounts for any variation in seed counts not explained by distance from parent. For example, high clumping could indicate that seedlings are constrained to specific habitat types within the study area (Comita et al., 2007b), or aggregated in gaps in the case of shade-intolerant species; indeed, some of the species with higher estimates of clumping for recruits compared to seeds (e.g., *A. blackiana*, *Cordia allidora*, *Cordia*

*bicolor*) are all highly light demanding during early regeneration and only become established in rare, high light gaps (Wright et al., 2003).

By assuming fixed dispersal and recruitment kernels at the species level, our model ignores intraspecific variation driven by local conditions, even though such variation may have both positive and negative effects on interspecific coexistence (Snell et al., 2019). Although we model the
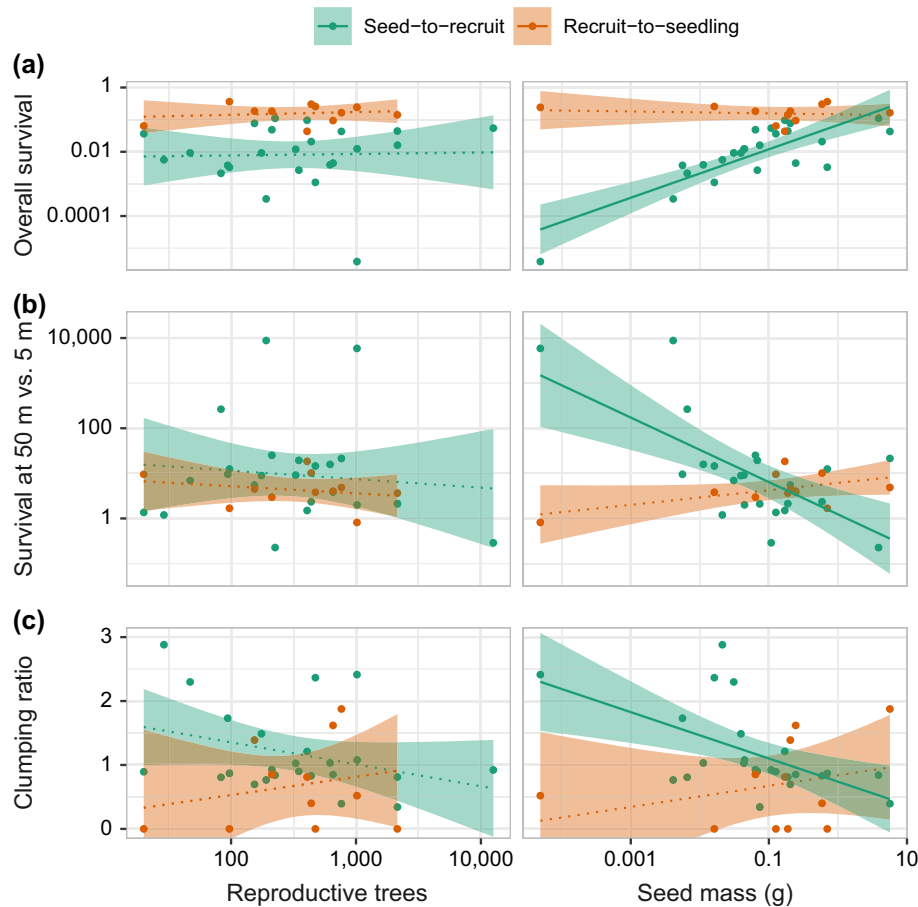
FIG. 5. (a) Overall survival rate, (b) relative survival at 50 vs. 5 m and (c) ratio of clumping factor ($\theta^{-1/2}$), calculated for the transition from seeds to new recruits and from recruits to 20-cm seedlings by species, as a function of the number of reproductive trees in the study area and seed mass. Points represent median multimodel estimates for individual species and each line shows the best linear fit, with the 95% confidence interval shown as shaded area. Dotted lines indicate non significant correlations.

average dispersal kernel across years, the results could be misleading if the inter annual variation in dispersal was correlated with that of fecundity, for example, if specialist animal dispersers behave differently in years of low and high seed production for a given species.

In this study, the establishment kernel for new recruits was based on distance to reproductive trees during the associated seed year, whereas the kernel for seedlings 20 cm and taller (which are often over a decade old) was based on contemporaneous adults. Comparing these kernels may thus also indicate the relative strength of distance-dependent mortality relative to a potential parent vs. any large conspecific individual. For some species (e.g., *Hirtella triandra*, *I. marginata* and *Quararibea asterolepis*), the pattern of relative survival for seed-to-recruit and recruit-to-seedling are similar. In other cases, the pattern of relative survival with distance in the recruit-to-seedling transition differs from that in the seed-to-recruit transition. For *A. blackiana*, *C. bicolor*, and *E. oerstediana*, the recruit-to-seedling survival is higher at shorter distances from a tree than seed-to-

recruit survival. This might be due to within-species pathogen specialization, which would have a greater effect near the mother tree relative to any conspecific adult (Eck et al., 2019, Gallery et al., 2007). For *Chrysophyllum cainito*, *Heisteria concinna*, and *Unonopsis pittieri*, seed-to-recruit survival was higher than recruit-to-seedling survival at short distances. This may indicate negative conspecific distance- or density-dependent mortality independent of genotype. Additional studies could examine the mechanisms underlying these patterns.

Contrary to many dispersal studies that emphasize the selection of a best kernel function for inference, we found that multiple kernels could fit each species' data and thus used model stacking to obtain multimodel predictions. This approach provides more robust model predictions with uncertainty estimates that include model selection error. However, the data requirements for precisely fitting dispersal kernels at the species level meant that we could only include a small fraction of the species at BCI, and thus limited the power of this study to make inference across species, for example, linking distance-

dependent survival to other species traits. To address these limitations, we would suggest the exploration of a multi species modeling approach, where dispersal models are fit to data from a group of species at once, with the models' parameters allowed to vary across species as random effects or based on the values of specific traits. Similar methods have been applied in the animal movement literature (Ovaskainen et al. 2019) for the joint movement modeling of bird species.

## Conclusion

Our study suggests that Hubbell patterns were the dominant recruitment pattern for the 24 species included. For most of these species, the strength of conspecific negative distance-dependent mortality at the seed-to-seedling transition stage is not sufficient on its own to result in spacing among conspecifics and potentially not sufficient to promote local coexistence among species. Therefore, maintenance of local diversity in this system likely requires that distance-dependent mechanisms, such as specialist natural enemies, significantly affect survival throughout the seedling stage. We were only able to include a small subset of the over 300 tree species that have been censused in the 50-ha Forest Dynamics Plot located on Barro Colorado Island, Panama (Condit, 1998). Future studies can examine whether these patterns are general among species of the plant community and determine the mechanisms underlying the recruitment patterns quantified here. In addition to conspecific negative distance/density-dependent mortality, other processes, such as habitat requirements of species, are an important driver of spatial patterns at these early stages of plant recruitment.

## Literature Cited

Beckman, N. G., et al. 2019. Advancing an interdisciplinary framework to study seed dispersal ecology. AoB Plants. https://doi.org/10.1093/aobpla/plz048

Beckman, N. G., and H. S. Rogers. 2013. Consequences of seed dispersal for plant recruitment in tropical forests: Interactions within the seedscape. Biotropica 45:666–681.

Betancourt, M. 2017. A conceptual introduction to Hamiltonian Monte Carlo. arXiv:1701.02434.

Bruijning, M., M. D. Visser, H. C. Muller-Landau, S. J. Wright, L. S. Comita, S. P. Hubbell, H. de Kroon, and E. Jongejans. 2017. Surviving in a cosexual world: A cost-benefit analysis of dioecy in tropical trees. American Naturalist 189:297–314.

Bullock, J. M., L. M. Gonzlez, R. Tamme, L. Gtzenberger, S. M. White, M. Prtel, and D. A. P. Hooftman. 2017. A synthesis of empirical plant dispersal kernels. Journal of Ecology 105:6–19.

Carpenter, B., A. Gelman, M. Hoffman, D. Lee, B. Goodrich, M. Betancourt, M. Brubaker, J. Guo, P. Li, and A. Riddell. 2017. Stan: A probabilistic programming language. Journal of Statistical Software. https://doi.org/10.18637/jss.v076.i01

Clark, J. S., E. Macklin, and L. Wood. 1998. Stages and spatial scales of recruitment limitation in southern Appalachian forests. Ecological Monographs 68:213–235.

Clark, J. S., M. Silman, R. Kern, E. Macklin, and J. Hille Ris Lambers. 1999. Seed dispersal near and far: patterns across temperate and tropical forests. Ecology 80:1475–1494.

Comita, L. S., S. Aguilar, R. Pérez, S. Lao, and S. P. Hubbell. 2007a. Patterns of woody plant species abundance and diversity in the seedling layer of a tropical forest. Journal of Vegetation Science 18:163–174.

Comita, L. S., R. Condit, and S. P. Hubbell. 2007b. Developmental changes in habitat associations of tropical trees. Journal of Ecology 95:482–492.

Comita, L. S., H. C. Muller-Landau, S. Aguilar, and S. P. Hubbell. 2010. Asymmetric density dependence shapes species abundances in a tropical tree community. Science 329:330–332.

Comita, L. S., S. A. Queenborough, S. J. Murphy, J. L. Eck, K. Y. Xu, M. Krishnadas, N. Beckman, and Y. Zhu. 2014. Testing predictions of the Janzen–Connell hypothesis: a meta-analysis of experimental evidence for distance- and density-dependent seed and seedling survival. Journal of Ecology 102:845–856.

Condit, R. 1998. Tropical forest census plots: Methods and results from Barro Colorado Island, Panama and a comparison with other plots. Springer-Verlag, Berlin, Germany.

Condit, R., S. Lao, R. Prez, S. Dolins, R. Foster, and S. Hubbell. 2012. Barro Colorado Forest census plot data. https://repository.si.edu/handle/10088/20925

Connell, J. H. 1971. On the role of natural enemies in preventing competitive exclusion in some marine animals and in rain forests. Pages 298–312 in P. J. den Boer and G. R. Gradwell, editors. Dynamics of populations. PUDOC, Wageningen, The Netherlands.

Detto, M. 2019. Bias in the detection of negative density dependence in plant communities. Ecology Letters. https://doi.org/10.1111/ele.13372

Eck, J. L. 2019. Evidence of within-species specialization by soil microbes and the implications for plant community diversity. Proceedings of the National Academy of Sciences of the United States of America. 116:201810767.

Gallery, R. E., J. W. Dalling, and A. E. Arnold. 2007. Diversity, host afnity, and distribution of seed-infecting fungi: a case study with cecropia. Ecology 88:582–588.

Gelman, A., and D. B. Rubin. 1992. Inference from iterative simulation using multiple sequences. Statistical Science 7:457–472.

Harms, K. E., S. J. Wright, O. Calderón, A. Hernández, and E. A. Herre. 2000. Pervasive density-dependent recruitment enhances seedling diversity in a tropical forest. Nature 404:493.

Howe, H. F., and M. Miriti. 2004. When seed dispersal matters. BioScience 54:651–660.

Hubbell, S. P. 1980. Seed predation and the coexistence of tree species in tropical forests. Oikos 35:214–229.

Hubbell, S. P., and R. B. Foster.1983. Diversity of canopy trees in a Neotropical forest and implications for conservation. Pages 25–41 *in* S. L. Sutton, T. C. Whitmore and A. C. Chadwick, editors. Tropical rain forest: Ecology and management. Blackwell Scientific Publications, Oxford, UK.

Hubbell, S., R. Foster, S. O'Brien, K. Harms, R. Condit, B. Wechsler, S. Wright, and S. Loo de Lao. 1999. Light gap disturbances, recruitment limitation, and tree diversity in a Neotropical forest. Science 283:554–557.

Janzen, D. H. 1970. Herbivores and the number of tree species in tropical forests. American Naturalist 104:501–528.

Lebrija-Trejos, E., P. B. Reich, A. Hernández, and S. J. Wright. 2016. Species with greater seed mass are more tolerant of conspecific neighbours: a key driver of early survival and future abundances in a tropical forest. Ecology Letters 19:1071–1080.

Leigh, J., G. Egbert, S. Rand, and D. M. Windsor, editors.1996. The ecology of a tropical forest: Seasonal rhythms and long-term changes. Second edition. Smithsonian Institution Press, Washington, D.C., USA.

Levin, S. A., H. C. Muller-Landau, R. Nathan, and J. Chave. 2003. The ecology and evolution of seed dispersal: a theoretical perspective. Annual Review of Ecology, Evolution, and Systematics 34:575–604.

Lin, Y. C., L. W. Chang, K. C. Yang, H. H. Wang, and I. F. Sun. 2011. Point patterns of tree distribution determined by habitat heterogeneity and dispersal limitation. Oecologia 165:175–184.

McCanny, S. 1985. Alternatives in parent–offspring relationships in plants. Oikos 45:148–149.

Muller-Landau, H. C., S. J. Wright, O. Caldern, R. Condit, and S. P. Hubbell. 2008. Interspecific variation in primary seed dispersal in a tropical forest. Journal of Ecology 96: 653–667.

Murphy, S. J., T. Wiegand, and L. S. Comita. 2017. Distance-dependent seedling mortality and long-term spacing dynamics in a Neotropical forest community. Ecology Letters 20:1469–1478.

Nathan, R., and R. Casagrandi. 2004. A simple mechanistic model of seed dispersal, predation and plant establishment: Janzen–Connell and beyond. Journal of Ecology 92: 733–746.

Nathan, R., and H. C. Muller-Landau. 2000. Spatial patterns of seed dispersal, their determinants and consequences for recruitment. Trends in Ecology and Evolution 15: 278–285.

Nathan, R., E. Klein, J. J. Robledo-Arnuncio, and E. Revilla. 2012. Dispersal kernels: a review. Pages 187–210 *in* J. Clobert, M. Baguette, T. G. Benton, and J. M. Bullock, editors. Dispersal ecology and evolution. Oxford University Press, Oxford, UK, book section 15.

Ovaskainen, O., D. L. Ramos, E. M. Slade, T. Merckx, G. Tikhonov, J. Pennanen, M. A. Pizo, M. C. Ribeiro, and J. M. Morales. 2019. Joint species movement modeling: how do traits inuence movements? Ecology 100:e02622.

Paton, S. 2007. 2006 Meteorological and hydrological summary for Barro Colorado Island. Smithsonian Tropical Research Institute, Panama City, Panama.

Perry, G. L. W., B. P. Miller, and N. J. Enright. 2006. A comparison of methods for the statistical analysis of spatial point patterns in plant ecology. Plant Ecology 187:59–82.

Ribbens, E., J. A. Silander, and S. W. Pacala. 1994. Seedling recruitment in forests: calibrating models to predict patterns of tree seedling dispersion. Ecology 75:1794–1806.

Ripley, B. D. 1977. Modelling spatial patterns. Journal of the Royal Statistical Society: Series B (Methodological) 39:172–212.

Schupp, E. W., P. Jordano, and J. Maria Gomez. 2010. Seed dispersal effectiveness revisited: a conceptual review. New Phytologist 188:333–353.

Snell, R. S., et al. 2019. Consequences of intraspecific variation in seed dispersal for plant demography, communities, evolution and global change. AoB Plants 11:plz016.

Swamy, V., J. Terborgh, K. G. Dexter, B. D. Best, P. Alvarez, and F. Cornejo. 2011. Are allseeds equal? Spatially explicit comparisons of seed fall and sapling recruitment in atropical forest. Ecology Letters 14:195–201.

Vehtari, A., A. Gelman, and J. Gabry. 2017. Practical Bayesian model evaluation using leave-one-out cross-validation and WAIC. Statistics and Computing 27:1413–1432.

Wiegand, T., I. Martinez, and A. Huth. 2009. Recruitment in tropical tree species: revealing complex spatial patterns. American Naturalist 174:E106–E140.

Wright, S. J., et al. 2010. Functional traits and the growth–mortality trade-off in tropical trees. Ecology 91:3664–3674.

Wright, S. J., and O. Calderon. 1995. Phylogenetic patterns among tropical owering phenologies. Journal of Ecology 83:937–948.

Wright, S. J., C. Carrasco, O. Calderon, and S. Paton. 1999. The El Niño Southern Oscillation, variable fruit production, and famine in a tropical forest. Ecology 80:1632–1647.

Wright, S. J., H. C. Muller-Landau, R. Condit, and S. P. Hubbell. 2003. Gap-dependent recruitment, realized vital rates, and size distributions of tropical trees. Ecology 84:3174–3185.

Wright, S. J., M. A. Jaramillo, J. Pavon, R. Condit, S. P. Hubbell, and R. B. Foster. 2005*a*. Reproductive size thresholds in tropical trees: variation among individuals, species and forests. Journal of Tropical Ecology 21:307–315.

Wright, S. J., H. C. Muller-Landau, O. Calderóon, and A. Hernandéz. 2005*b*. Annual and spatial variation in seedfall and seedling recruitment in a Neotropical forest. Ecology 86:848–860.

Yao, Y., A. Vehtari, D. Simpson, and A. Gelman. 2018. Using stacking to average Bayesian predictive distributions. Bayesian Analysis 13:917–1007.

## Supporting Information

Additional supporting information may be found in the online version of this article at http://onlinelibrary.wiley.com/doi/10.1002/ecy.2926/suppinfo

## Data Availability

Additional material (R and Stan code files) is provided on Zenodo: http://doi.org/10.5281/zenodo.3418728